

# Effect of Surfactants on the Film Drainage

Krassimir D. Danov,<sup>1</sup> Dimitrina S. Valkovska, and Ivan B. Ivanov

Laboratory of Thermodynamics and Physicochemical Hydrodynamics, Faculty of Chemistry, Sofia University, 1 J. Bourchier Ave., 1164 Sofia, Bulgaria

Received May 19, 1998; accepted November 9, 1998

**Drainage of a partially mobile thin liquid film between two deformed and nondeformed gas bubbles with different radii is studied. The lubrication approximation is used to obtain the influence of soluble and insoluble surfactants on the velocity of film thinning in the case of quasi-steady state approach. The material properties of the interfaces (surface viscosity, Gibbs elasticity, surface diffusivity, and/or bulk diffusivity) are taken into account. In the case of deformed bubbles the influence of the meniscus is illustrated assuming simple approximated shape for the local film thickness. Simple analytical solutions for large and small values of the interfacial viscosity, and for deformed and nondeformed bubbles, are derived. The correctness of the boundary conditions used in the literature is discussed. The numerical analysis of the governing equation shows the region of transition from partially mobile to immobile interfaces. Quantitative explanation of the following effects is proposed: (i) increase of the mobility due to increasing bulk and surface diffusivities; (ii) role of the surface viscosity, comparable to that of the Gibbs elasticity; and (iii) significant influence of the meniscus on the film drainage due to the increased hydrodynamic resistance.** © 1999 Academic Press

**Key Words:** thin liquid films; drainage velocity; influence of surfactant; mobility of interfaces; bubbles; deformable interfaces.

## 1. INTRODUCTION

The stability of emulsions and foams plays a crucial role in various chemical technologies (1, 2). There have been numerous attempts to formulate simple rules connecting the foam and emulsion stability with the surfactant properties: the Bancroft rule (3); Griffin's criterion (4), which introduces the concept of the hydrophilic–lipophilic balance (HLB); the phase inversion temperature (PIT) rule of Schinoda and Friberg (5); etc. New interpretation of the Bancroft rule, taking into account the dynamic process of film drainage between the emulsion droplets, was given by Ivanov (6). Hence the detailed study of the surfactant influence on the velocity of film thinning is a starting point for many publications in the literature.

Plateau (7) showed that some surfactants strongly retard drainage from foam films and significantly increase their lifetime. Due to the process of film thinning the interfaces of an equilibrium surfactant solution are disturbed. The equilibrium is restored either by adsorption from the bulk phase or by

surface convection and diffusion, driven by the gradient of interfacial tension (Marangoni effect, see Ref. 8) in interplay with a specific interfacial viscous friction (the so-called Boussinesq effect, see Ref. 9). In order to estimate these effects many authors consider the *problem of motion of deformable bubbles and drops* each toward the other. In the literature two methods for solving this problem are available: numerical investigation of *deformable drops motion*, when the whole process of dimple formation and growth depends on the initial condition and interfacial properties (10, 11), and analytical and numerical investigation of almost *plane-parallel film thinning* in quasi-steady state approach (12–17). All experimental results showed that the complete process of drainage of a thin liquid film has five stages, depending on the hydrodynamic and intermolecular interactions (6, 18). However, the time limiting factors for coalescence or flocculation are the approach of drops as nondeformed spheres (earliest stage), and the drainage of the formed film between the drops (if it appears). When two bubbles or drops approach each other, at high distances their interfaces slightly deform and at a given thickness (the so-called inversion thickness) the interfacial shape changes from convex to concave: a *dimple is formed*. All numerical models of deformable drops motion investigated the growing of this formation. Unfortunately, this is not a real experimental situation, because of *instability of the dimple*: it actually flows out soon after the formation and an almost plane-parallel film is formed (6, 19). This film, due to the action of disjoining pressure and hydrodynamic resistance, thins down to the final critical thickness without changing its radius,  $R$ , with a given geometry of the meniscus (20). Therefore, models of an infinite plane-parallel film describe qualitatively well most of the available experimental data. This physical picture takes place if the drops are relatively large (above 50–100  $\mu\text{m}$  for buoyancy driven coalescence). On the contrary, due to the high capillary pressure, small drops keep their shape practically spherical up to the moment of flocculation or coalescence. Below we will investigate separately the influence of surfactants on the drainage in the following two cases: (A) *spherical nondeformed drops* (bubbles), at the earlier stage of the drop's approach or for small drop sizes (see Fig. 1a and Section 3) and (B) the later stage, when the almost *plane-parallel film* is already formed, *bounded by the meniscus* region (see Fig. 1b and Section 4). We will not discuss in this paper the case of pure liquid phases (for literature review see Ref. 21).

The first solution of the problem for approaching of two

<sup>1</sup> To whom correspondence should be addressed. Fax: (359) 2 962 5643. E-mail: Krassimir.Danov@lph.bol.bg.

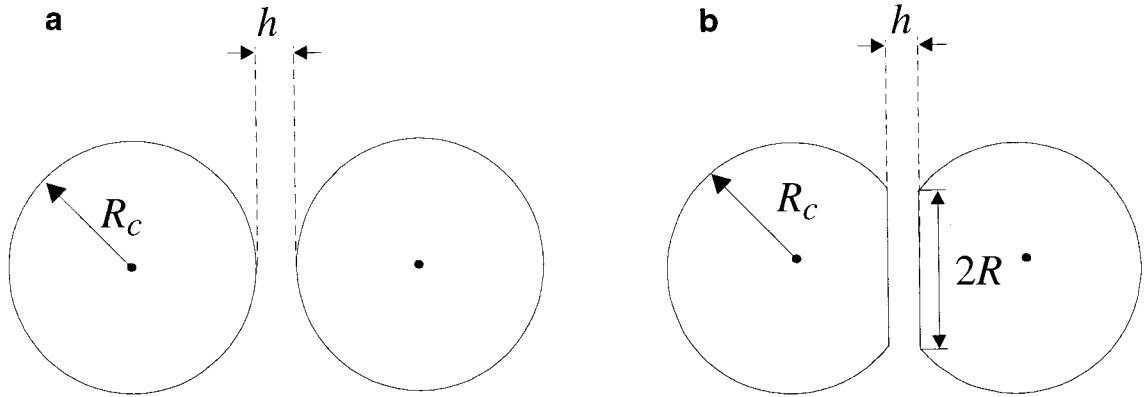


**FIG. 1.** Sketch of two bubbles of radius  $R_c$  separated at a surface-to-surface distance  $h$ . (a) For large  $h$  the bubbles are spherical; (b) for small  $h$  the bubbles are deformed and a plane-parallel film with radius  $R$  surrounded by a meniscus appears.

rigid spherical particles was obtained by Taylor (22). For a long time the Taylor formula for the velocity of thinning was used in order to calculate the flocculation rate of suspensions. In the case of two spherical drops when the surfactants are soluble only in the continuous phase simple asymptotic expression was derived by Ivanov *et al.* (14). It takes into account the influence of Gibbs elasticity and bulk and surface diffusivities, but the effects of the interfacial viscosity and the disjoining pressure were not included in computations.

The model for thin liquid film drainage has been proposed by Reynolds (23), who solved the problem for the approach of two plane-parallel circular disks with tangentially immobile surfaces. If there is a contribution of the disjoining pressure, the corresponding formula was derived by Scheludko (24). Ivanov (6) discussed the effect of surface mobility on the drainage and rupture of plane-parallel thin liquid films. Many authors (12, 13, 15, 25, 26) treat the hydrodynamics of thin liquid foam films. They showed that the surface elasticity and viscosity strongly reduce the interfacial mobility. The corresponding models for *emulsion* films, for which the surfactant is soluble only in the continuous phase are described in Refs. 6, 16, 27, 28. It was shown therein that in the presence of surfactants the energy dissipates mainly in the film region, and the emulsion films behave just as foam films. These studies have two problems, which are not solved. The first one is connected with influence of the meniscus on the velocity of thinning (the model of infinite film does not contain the meniscus region). The second problem concerns the correctness of the boundary conditions at the film ring. The viscous friction in a real system is a sum of the friction in the film and in the meniscus region, and as was shown in Ref. 21, for tangentially immobile interfaces, these two effects can be of the same order of magnitude. On the other hand, in the tangential stress boundary condition the interfacial viscous term contains the second derivative of the velocity on the radial coordinate. Therefore, boundary conditions at the film center and at the film ring are needed. However, in the models of infinite plane-parallel film the boundary conditions at the film ring are unknown. The boundary conditions used in the literature are different, based on the intuition of the authors, and the final results are not exact from the physical viewpoint (12, 13, 16)

(for additional discussions, see Sections 4.2 and 4.3). The solving of the corresponding problem for the whole film thinning and profile evolution can answer this question. Malhotra and Wasan (29) extended the applicability of the Reynolds model by accounting for the flow in the Plateau borders for films with tangentially immobile interfaces.

In this work we present a solution of the problem of drainage of a partially mobile thin liquid film between two deformed and nondeformed gas bubbles with different radii. In Section 2 a mathematical model based on the lubrication approximation and quasi-steady state assumption is formulated to derive the final governing equations for surface velocity and the film drainage velocity. This is followed by a study of the problem for two nondeformed bubbles (Section 3), when analytical formulae in the case of large and small surface viscosity effect can be obtained. The investigation of the influence of material properties on the velocity of thinning of films with a given geometry is presented in Section 4. Therein the influence of surfactants and the meniscus region are dealt with, and the comparison between our model and the model of Ivanov *et al.* (12) and Singh *et al.* (13) is illustrated.

## 2. MATHEMATICAL MODEL

We consider a thin viscous liquid layer between two gas bubbles, which flows out due to their approach under the action

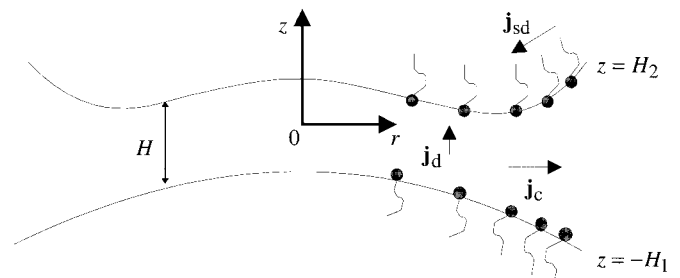


**FIG. 2.** Schematic picture of a thin liquid film between two deformed bubbles. The cylindrical coordinate system is  $Orz$ . The surfactant bulk and surface diffusion fluxes are respectively  $\mathbf{j}_d$  and  $\mathbf{j}_{sd}$ . The convection surfactant flux at the interface is  $\mathbf{j}_c$ .

of the external force,  $F$  (see Fig. 2). The problem is described in a cylindrical coordinate system,  $Orz$ , where the bubble interfaces are defined as  $z = \mp H_k(r, t)$ ,  $k = 1, 2$ , and  $t$  is the time. In the literature (12–14, 19, 29) the lubrication approximation is used for the solution of the governing equation. The general frame for this approximation is given by: (i) *small Reynolds number*, (ii) *small Peclet number*, (iii) *small film thickness* compared to the characteristic bubble radius, and (iv) *small slope of the interfaces*. In the lubrication approximation the pressure in the continuous phase depends only on the radial coordinate,  $r$ , and time,  $t$ :  $P = P(r, t)$ . The distribution of the radial component of the velocity,  $v_r$ , was calculated (14) to be

$$v_r = \frac{(z + H_1)(z - H_2)}{2\eta} \frac{\partial P}{\partial r} + \frac{H_2 - z}{H} U_1 + \frac{z + H_1}{H} U_2, \quad [1]$$

where  $H = H_2 + H_1$  is the local thickness of the film,  $\eta$  is the dynamic viscosity, and  $U_k$  is the component of the surface velocity, respectively, at the film interface  $z = \mp H_k(r, t)$ ,  $k = 1, 2$  (see Fig. 2).

From (14) the integrated bulk continuity equation can be written in the following form:

$$\frac{\partial H}{\partial t} + \frac{1}{r} \frac{\partial}{\partial r} (r H U_a) = 0. \quad [2]$$

In Eq. [2] the average velocity  $U_a$  is a sum of the Couette and the Poiseuille average velocities

$$U_a = \frac{1}{H} \int_{-H_1}^{H_2} v_r dz = \frac{U_1 + U_2}{2} - \frac{H^2}{12\eta} \frac{\partial P}{\partial r}. \quad [3]$$

The boundary condition for the balance of surface excess linear momentum takes into account the influence of the surface tension gradients (capillary and Marangoni effects) and the surface viscosity (Boussinesq effect). In the lubrication approximation the tangential stress boundary conditions at the film interfaces are simplified to

$$(-1)^k \eta \frac{\partial v_r}{\partial z} = \frac{\partial \sigma}{\partial r} + \eta_s \frac{\partial}{\partial r} \left[ \frac{1}{r} \frac{\partial}{\partial r} (r U_k) \right] \quad \text{at } z = \mp H_k, \quad [4]$$

where  $\sigma$  is the interfacial tension,  $\eta_s = \eta_{sh} + \eta_{dil}$  is the total surface viscosity, defined as a sum of the interfacial shear,  $\eta_{sh}$ , and dilatational,  $\eta_{dil}$ , viscosities, and  $k = 1, 2$ . We assume also that (v) *the interfacial properties of the two surfaces are the same*, because of the uniform distribution of the surfactant concentration along the  $z$  coordinate (the leading order of surfactant concentration depends on the  $r$  coordinate and time,

see Eqs. [6] and [7] below). If we substitute the general solution [1] into the boundary conditions [4] and add the resulting relationships we can derive the following condition,

$$\frac{H}{2} \frac{\partial P}{\partial r} = \frac{1}{2} \frac{\partial \sigma}{\partial r} + \eta_s \frac{\partial}{\partial r} \left[ \frac{1}{r} \frac{\partial}{\partial r} (r U) \right], \quad [5]$$

where the mean surface velocity is  $U = (U_1 + U_2)/2$ .

In order to close the system [2], [3], and [5] one has to solve the diffusion problem. For thin liquid films the Peclet number is a small parameter and the bulk surfactant concentration  $c$  depends weakly on the vertical coordinate  $z$ :  $c = c_s(r, t) + c_d(z, r, t)$ , where  $c_s \gg c_d$ . Therefore, in a first order approximation with respect to the Peclet number the diffusion equation in the film phase can be written in the following form,

$$\frac{\partial c_s}{\partial t} + v_r \frac{\partial c_s}{\partial r} - \frac{D}{r} \frac{\partial}{\partial r} \left( r \frac{\partial c_s}{\partial r} \right) = D \frac{\partial^2 c_d}{\partial z^2}, \quad [6]$$

where  $D$  is the bulk diffusion coefficient and the leading order of the surfactant concentration is  $c_s(r, t)$ . It was proved in the literature (19) that for the film thinning the diffusion-controlled adsorption processes are more important than the adsorption under barrier control. Therefore, we will consider here only (vi) *diffusion-controlled adsorption* and  $c_s(r, t)$  will be assumed equal to the subsurface concentration at both interfaces. Then after integrating the diffusion equation [6] over  $z$  from  $-H_1$  to  $H_2$  the leading order of the diffusion fluxes at the interfaces reads

$$H \frac{\partial c_s}{\partial t} + H U_a \frac{\partial c_s}{\partial r} - \frac{DH}{r} \frac{\partial}{\partial r} \left( r \frac{\partial c_s}{\partial r} \right) = D \left( \frac{\partial c_d}{\partial z} \Big|_{z=H_2} - \frac{\partial c_d}{\partial z} \Big|_{z=-H_1} \right). \quad [7]$$

If we multiply Eq. [2] with  $c_s$  and add the result to Eq. [7], we obtain

$$\begin{aligned} \frac{\partial}{\partial t} (H c_s) + \frac{1}{r} \frac{\partial}{\partial r} (r H U_a c_s) - \frac{DH}{r} \frac{\partial}{\partial r} \left( r \frac{\partial c_s}{\partial r} \right) \\ = D \left( \frac{\partial c_d}{\partial z} \Big|_{z=H_2} - \frac{\partial c_d}{\partial z} \Big|_{z=-H_1} \right). \end{aligned} \quad [8]$$

The balance of surfactant species in the case of diffusion-controlled adsorption at the film interfaces reads

$$\begin{aligned} \frac{\partial \Gamma}{\partial t} + \frac{1}{r} \frac{\partial}{\partial r} (r U_k \Gamma) - \frac{1}{r} \frac{\partial}{\partial r} \left( r D_s \frac{\partial \Gamma}{\partial r} \right) \\ = D (-1)^{k+1} \frac{\partial c_d}{\partial z} \Big|_{z=\mp H_k} + D \frac{\partial H_k}{\partial r} \frac{\partial c_s}{\partial r}, \end{aligned} \quad [9]$$

where  $\Gamma$  and  $D_s$  are the adsorption and the surface diffusion coefficient at the interface  $z = \mp H_k$  ( $k = 1, 2$ ), respectively. Finally, from the surfactant species balance [9] and from the integrated surfactant mass balance [8] one finds the total mass balance equation

$$\frac{\partial}{\partial t} (2\Gamma + Hc_s) = -\frac{1}{r} \frac{\partial}{\partial r} \times \left[ r \left( 2\Gamma U + Hc_s U_a - 2D_s \frac{\partial \Gamma}{\partial r} - DH \frac{\partial c_s}{\partial r} \right) \right]. \quad [10]$$

Here we wish to point out that the relationship [2] in Ref. 13 is erroneous, because the coefficient  $\frac{1}{2}$  therein must be  $\frac{1}{3}$ . This makes the comparison of most of the numerical results below and those obtained in Ref. 13 impossible.

The problem [2], [3], [5], and [10] has no analytical solution, because of the strong nonlinear dependence of the surface tension and adsorption on the subsurface concentration. In most of the publications in the literature (for detailed literature review see Ref. 19) the following assumptions are used: (vii) *small deviation from equilibrium*

$$c_s = c_0 + \delta c, \quad \Gamma = \Gamma_0 + \delta \Gamma, \quad [11]$$

where  $c_0$  and  $\Gamma_0$  are the equilibrium values and  $\delta c$  and  $\delta \Gamma$  are small deviations from the equilibrium values of the subsurface concentration and adsorption; (viii) *quasi-steady-state assumption*—all variables depend implicitly on time through the local film thickness. Then from assumption (vii) and the total mass balance equation [10] the gradient of the adsorption can be obtained. After substitution into Eq. [5] the final form of the tangential stress boundary condition reads (see Refs. 14 and 19)

$$\frac{H}{2} \frac{\partial P}{\partial r} = -E_G \left[ D_s + D \frac{H}{2} \left( \frac{\partial c}{\partial \Gamma} \right)_0 \right]^{-1} U + \eta_s \frac{\partial}{\partial r} \left[ \frac{1}{r} \frac{\partial}{\partial r} (rU) \right]. \quad [12]$$

The Gibbs elasticity,  $E_G$ , appearing in [12] is defined by the relationship  $E_G \equiv -\Gamma_0 (\partial \sigma / \partial \Gamma)_0$ . From the assumption (viii) the velocity of film thinning,  $V = -\partial H / \partial t$ , does not depend on the radial coordinate  $r$ . Hence, the integrated mass balance equation [2], in combination with Eq. [3], has the following first integral:

$$\frac{\partial P}{\partial r} = \frac{12\eta}{H^2} \left( U - \frac{Vr}{2H} \right). \quad [13]$$

Finally, from [12] and [13] the following second order differ-

ential equation for the distribution of the surface velocity,  $U$ , is obtained

$$\eta_s \frac{\partial}{\partial r} \left[ \frac{1}{r} \frac{\partial}{\partial r} (rU) \right] - \frac{6\eta U}{H} - \frac{E_G U}{D_s + \frac{D}{2} \left( \frac{\partial c}{\partial \Gamma} \right)_0 H} = -\frac{3\eta Vr}{H^2}, \quad [14]$$

with the boundary conditions of vanishing velocity,  $U$ , at the film origin,  $r = 0$  and at  $r$  going to infinity (the meniscus region).

The film between the bubbles thins due to the action of the external force (for example the buoyancy force),  $F$ , which in the quasi-steady state assumption is balanced by the hydrodynamic drag force and intermolecular forces. Hence, in the lubrication approximation we obtain

$$F = 2\pi \int_0^\infty (P + \Pi - P_m) r dr, \quad [15]$$

where  $\Pi$  is the disjoining pressure and  $P_m$  is the pressure at infinity in the meniscus region. Knowing the film profile and the type of intermolecular interactions (van der Waals, electrostatic, steric, etc., disjoining pressure), the external force can be connected with the hydrodynamic drag force acting on the bubbles,  $F_{hd}$  (see Ref. 20). After substitution of [13] into [15] and transformation of the resulting integrals, the relationship between the velocity of film thinning,  $V$ , and the hydrodynamic drag force,  $F_{hd}$ , is derived:

$$F_{hd} \equiv F - 2\pi \int_0^\infty \Pi r dr = 6\pi\eta V \int_0^\infty \frac{r^3}{H^3} dr - 12\pi\eta V \int_0^\infty \left( \frac{r}{H} \right)^2 \frac{U}{V} dr. \quad [16]$$

In order to compute numerically the problem [14] and [16] appropriate scaling of the parameters is needed. We will use the natural scales widely used in the literature (30):  $U = V\sqrt{R_c h} \tilde{U} / (2h)$ ;  $r^2 = R_c h x^2$ ; and  $H = h\tilde{H}$ , where the dimensionless velocity, radial coordinate, and local film thickness are  $\tilde{U}$ ,  $x$ , and  $\tilde{H}$ , respectively. In these scales  $h$  is the minimal distance between the surfaces and  $R_c$  is the mean value of the radii  $R_{c,1}$  and  $R_{c,2}$  of the nondeformed parts of the bubbles:  $R_c = 2R_{c,1}R_{c,2} / (R_{c,1} + R_{c,2})$  (see Fig. 1). Using the dimensionless numbers introduced in Ref. 13 for describing the dependence of the thinning velocity on the physical parameters is not convenient, because these numbers were defined as functions of the thickness  $h$ , which depends on time. Hence, these numbers change by orders of magnitude for a given film in a process of its thinning. Here we will use the dimensionless

surface viscosity and bulk diffusivity numbers,  $N_{sv}$  and  $b$ , and the characteristic surface diffusion length,  $h_s$ :

$$N_{sv} \equiv \frac{\eta_s}{6\eta R_c}, \quad b \equiv \frac{3\eta D}{E_G} \left( \frac{\partial c}{\partial \Gamma} \right)_0, \quad h_s \equiv \frac{6\eta D_s}{E_G}. \quad [17]$$

The parameters defined via Eqs. [17] do not depend on the thickness  $h$ . They can have values which differ in several orders of magnitude depending on the type of surfactants and the surfactant concentration. The surface viscosity number,  $N_{sv}$ , has the following characteristic values for water solution of ionic, nonionic, and high molecular weight surfactants close to the critical micellar concentration (CMC): for ionic and nonionic surfactants  $\eta_s \approx 10^{-6}$  msPa and for  $R_c = 2$  mm we calculate  $N_{sv} = 0.1$ , in contrast for  $R_c = 20 \mu\text{m}$  we have  $N_{sv} = 10$ ; for high molecular weight surfactants the typical value of the surface viscosity is  $\eta_s \approx 5 \times 10^{-3}$  msPa and for  $R_c = 2$  mm –  $N_{sv} = 500$ , while for  $R_c = 20 \mu\text{m}$  –  $N_{sv} = 5 \times 10^4$ . With decreasing of the surfactant concentration the surface viscosity decreases and the respective number,  $N_{sv}$ , also decreases. In order to estimate the values of the bulk diffusivity number,  $b$ , and the characteristic surface diffusion length,  $h_s$ , we will use the common Langmuir isotherm,

$$\frac{\Gamma_0}{\Gamma_\infty} = \frac{c_0}{c_L + c_0}, \quad \left( \frac{\partial \Gamma}{\partial c} \right)_0 = \frac{\Gamma_\infty c_L}{(c_L + c_0)^2}, \quad E_G = \frac{k_B T \Gamma_0}{1 - \Gamma_0/\Gamma_\infty}, \quad [18]$$

where  $\Gamma_\infty$  is the saturation adsorption,  $c_L$  is a constant parameter of the adsorption isotherm, related to the energy of adsorption per molecule,  $T$  is the temperature, and  $k_B$  is the Boltzmann constant. Then the corresponding relationships for  $b$  and  $h_s$  read

$$b = \frac{3\eta D}{k_B T \Gamma_0} \frac{c_L}{\Gamma_\infty} \left( 1 - \frac{\Gamma_0}{\Gamma_\infty} \right)^{-1}, \quad h_s = \frac{6\eta D_s}{k_B T \Gamma_0} \left( 1 - \frac{\Gamma_0}{\Gamma_\infty} \right). \quad [19]$$

From Eqs. [19] it is seen that for very low surfactant concentrations both parameters have high values and when the concentration is close to CMC  $b$  is a very small parameter for all types of surfactant, but  $h_s/h$  can drop to a final value for small thicknesses.

The dimensionless form of the tangential stress boundary condition [14] and the relationship for the total force [16] have the following final form,

$$N_{sv} \frac{\partial}{\partial x} \left[ \frac{1}{x} \frac{\partial}{\partial x} (x\tilde{U}) \right] - \left( \frac{1}{\tilde{H}} + \frac{h}{h_s + bh\tilde{H}} \right) \tilde{U} = -\frac{x}{\tilde{H}^2}, \quad [20a]$$

$$1 = \frac{V}{V_{GT}} \left[ 4 \int_0^\infty \frac{x^3}{\tilde{H}^3} dx - \int_0^\infty \left( \frac{2x}{\tilde{H}} \right)^2 \tilde{U} dx \right], \quad [20b]$$

where  $V_{GT} = 2hF_{hd}/(3\pi\eta R_c^2)$  is the generalization of Taylor's result for the rate of thinning of a fluid layer between two rigid spheres (22), which takes into account the influence of the disjoining pressure (the hydrodynamic drag force,  $F_{hd}$ , is different from the external force,  $F$ , see Eq. [16]).

### 3. INFLUENCE OF SURFACTANTS ON THE APPROACHING VELOCITY OF TWO BUBBLES

In this section we present the solution of the system [20] in the case of large distances between the bubbles or small radii, when the bubbles are slightly deformed (case A in the Introduction). Analytical formulas are obtained in the particular cases of small and large surface viscosity. The numerical results are described in Section 3.3.

#### 3.1. Exact Solution of the Problem

If the capillary pressure is high enough the bubble shapes are close to spherical. In the frames of the lubrication approximation the local film thickness is approximated by the parabolic function  $\tilde{H} = 1 + x^2$ . This profile is the leading order solution of the boundary condition for the pressure; therefore, the solution of the corresponding hydrodynamic problem gives the leading order of the velocity of bubble approach. The wide range of  $x$  from zero to infinity makes the numerical solution of the equation [20a] with a high precision impossible. To overcome these difficulties, we will introduce a new variable,  $x = \tan(\theta/2)$ , which transforms the infinite range to the finite interval  $[0, \pi]$ , where the infinity point is transformed to  $\theta = \pi$ , and the zero point is  $\theta = 0$ . With the new variable, taking into account the approximate film profile,  $\tilde{H} = 1/\cos^2(\theta/2)$ , the final form of Eq. [20a] is reduced to

$$N_{sv} \sin^2(\theta) \frac{\partial^2 \tilde{U}}{\partial \theta^2} + N_{sv} \sin(\theta) \cos(\theta) \frac{\partial \tilde{U}}{\partial \theta} - \left[ N_{sv} + \sin^2(\theta/2) + \frac{h \sin^2(\theta/2)}{h_s \cos^2(\theta/2) + hb} \right] \tilde{U} = -\frac{1}{2} \sin(\theta) \sin^2(\theta/2). \quad [21]$$

Because of the boundary conditions at  $\theta = 0$  and  $\theta = \pi$  the solution of [21] can be presented as a Fourier series,  $\tilde{U} = \sum_{k=1}^\infty a_k \sin(k\theta)$ , where  $a_k$  are the coefficients depending implicitly on time through  $h$ . The details of the numerical procedure for calculations according to Eq. [21] are given in Appendix A. If we substitute the general form of the solution into Eq. [21b] the expression for approaching velocity reads

$$1 = \frac{V}{V_{GT}} \left[ 1 - \sum_{k=0}^\infty \frac{2}{(2k+1)} a_{2k+1} + \sum_{k=1}^\infty \frac{4k}{4k^2-1} a_{2k} \right]. \quad [22]$$

The numerical results and discussions are given in Section 3.3.

### 3.2. Analytical Solutions in the Cases of Small and Large Surface Viscosity Number

When the surface viscosity is very low we can neglect all terms proportional to  $N_{sv}$ . Then directly from Eqs. [20a] and [20b] the following analytical solution can be derived:

$$\tilde{U} = \frac{x}{(1+x^2)^2} \left[ \frac{1}{1+x^2} + \frac{h}{h_s + bh(1+x^2)} \right]^{-1}, \quad [23a]$$

$$\frac{V}{V_{GT}} = \frac{h_s}{2h} \left\{ \left[ \frac{h(1+b)}{h_s} + 1 \right] \ln \left[ \frac{h_s}{h(1+b)} + 1 \right] - 1 \right\}^{-1}. \quad [23b]$$

The formulae [23b] were first derived by Ivanov *et al.* (14). The particular cases of large and small surface diffusion effects were investigated therein (see Eqs. [61] and [63] in Ref. 14). Using the asymptotic analysis of the problem [20] the first order corrections of the approaching velocity proportional to the surface viscosity number  $N_{sv}$  have been obtained by us. The analytical results for the next term in the expansion are given in Appendix C.

In the opposite case of large surface viscosity effect compared to the bulk and surface diffusion effects ( $N_{sv} \gg 1$ ,  $bN_{sv} \gg 1$ , and  $h_s N_{sv}/h \gg 1$ ) the surfactants influence the liquid flow only through the surface viscosity. (It is important to note that the surface viscosity influences the process of bubbles approach only when the interfaces are mobile, i.e., the assumptions  $bN_{sv} \gg 1$  and  $h_s N_{sv}/h \gg 1$  are not valid for small values of  $b$  and  $h_s/h$ , when the interfaces are immobile because of the influence of Gibbs elasticity.) Therefore, in this case the damping effects of Gibbs elasticity and surface viscosity are coupled and they cannot be separated. The analytical solution of Eqs. [20a] and [20b] can be calculated to be

$$\tilde{U} = \frac{1}{4N_{sv}x} \ln(1+x^2), \quad [24a]$$

$$\frac{V}{V_{GT}} = \frac{2N_{sv}}{2N_{sv} - 1}. \quad [24b]$$

From [24b] it is seen that the approaching velocity,  $V$ , is close to the generalized Taylor velocity,  $V_{GT}$ , and from the experimental results it is possible to fit the value of surface viscosity. The surface velocity,  $\tilde{U}$ , is very small: it is inversely proportional to the surface viscosity number,  $N_{sv}$ . The distance at which the surface velocity has a maximum,  $x_{\max} = 1.9803$ , does not depend on the surfactants and the maximum value at this point is  $\tilde{U}_{\max} = 0.20119/N_{sv}$ . It is interesting to note the very long tail asymptotic of the surface velocity: at infinity it decreases as  $\tilde{U} \propto \ln(x)/x$ .

### 3.3. Numerical Results and Discussions

The numerical procedure used for calculations given below is described in Appendix A. The influence of surfactants on the

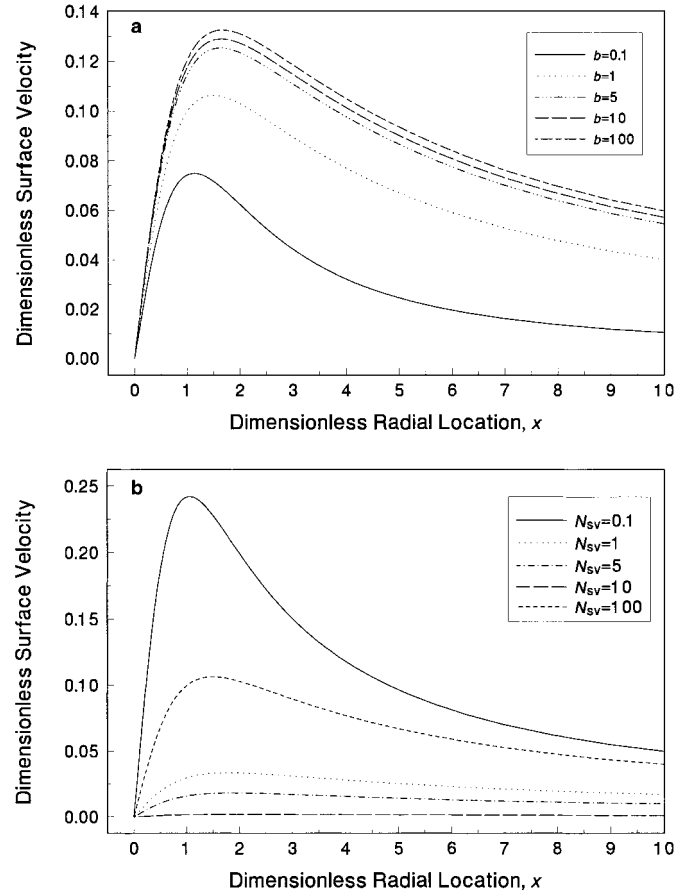


**FIG. 3.** Dimensionless surface velocity,  $\tilde{U}$ , distribution at a given distance  $h$ : (a) for  $N_{sv} = 1$ ,  $h_s/h = 1$ , and different values of the parameter  $b$ ; (b) for  $b = 1$ ,  $h_s/h = 1$ , and different values of the parameter  $N_{sv}$ .

interfacial mobility is demonstrated in Fig. 3. If the surface viscosity,  $\eta_s$ , surface diffusion coefficient,  $D_s$ , and the distance between the bubbles,  $h$ , are constants, then with increasing of the bulk diffusivity the surface mobility increases (see Fig. 3a). This fact is due to the faster saturation of the interface from the bulk, which leads to suppression of the Marangoni effect. The distance at which the dimensionless surface velocity has a maximum slightly increases and the interface is mobile in a wide region. The effect of surface viscosity on the interfacial mobility is well pronounced (see Fig. 3b, where the bulk and surface diffusivities are kept constants and only the surface viscosity numbers are varied). In contrast with Fig. 3a the peak of the velocity distribution is narrower and at infinity the velocity decreases faster than in Fig. 3a. The maximum of the velocity is shifted to the asymptotic value of  $x_{\max} = 1.9803$  with an increase of the surface viscosity number.

In order to clarify how the approaching velocity is influenced by the physical parameters of the system we calculate the mobility factor,  $V/V_{GT}$ , for different values of  $b$ ,  $h_s/h$ , and  $N_{sv}$ . In Fig. 4 we choose the value of  $h_s/h$  to be 1 and plot the dimensionless drainage velocity,  $V/V_{GT}$ , as a function of surface viscosity and bulk diffusion numbers. The increasing of

the surface viscosity in all cases of mobile interfaces leads to a decrease of the approaching velocity (see Fig. 4a). This effect is more pronounced for higher values of the bulk diffusivity, where due to the faster saturation of the interfaces the surface gradient of the adsorption is suppressed and the Marangoni effect is not so big; i.e., the effect of elasticity is smaller than that of surface viscosity. The decreasing of the velocity is achieved for lower values of  $b$  when the surface viscosity number increases (compare Figs. 4a and 4b). In contrast the fast approach of the film interfaces at  $N_{sv} = 0.01$  and  $b = 100$  may be due to the inapplicability of the lubrication approximation for modeling the hydrodynamic resistance of film between fully mobile interfaces. Then the full Stokes equations have to be solved (see Ref. 30). When  $b \rightarrow 0$  the role of bulk diffusivity is negligible and the surfactants behave as insoluble (for absolutely insoluble surfactant monolayers  $b = 0$ ). Then only the surface diffusivity plays a role for the velocity of approach. In Fig. 5 the mobility factor has been calculated keeping the surface viscosity constant. The higher the dimensionless parameter  $h_s/h$  the faster the bubbles approach. Therefore, for high surface diffusivity or small film thickness the mobility of interfaces increases. This conclusion is stronger

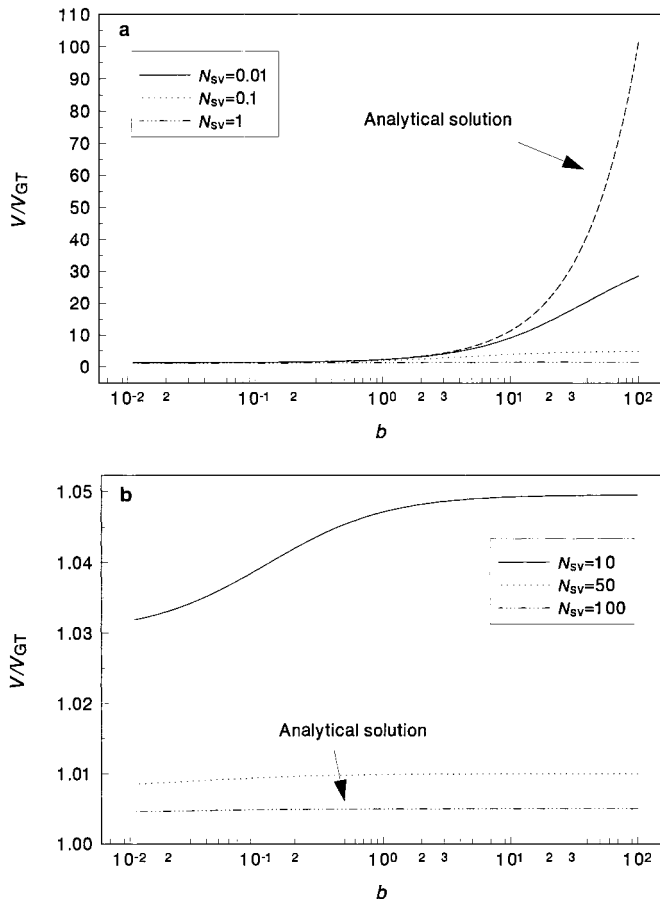


**FIG. 4.** Variation of the mobility factor,  $V/V_{GT}$ , with the bulk diffusion parameter  $b$ : (a) for  $h_s/h = 1$  and low and moderate values of the parameter  $N_{sv}$ ; (b) for  $h_s/h = 1$  and high values of the parameter  $N_{sv}$ .

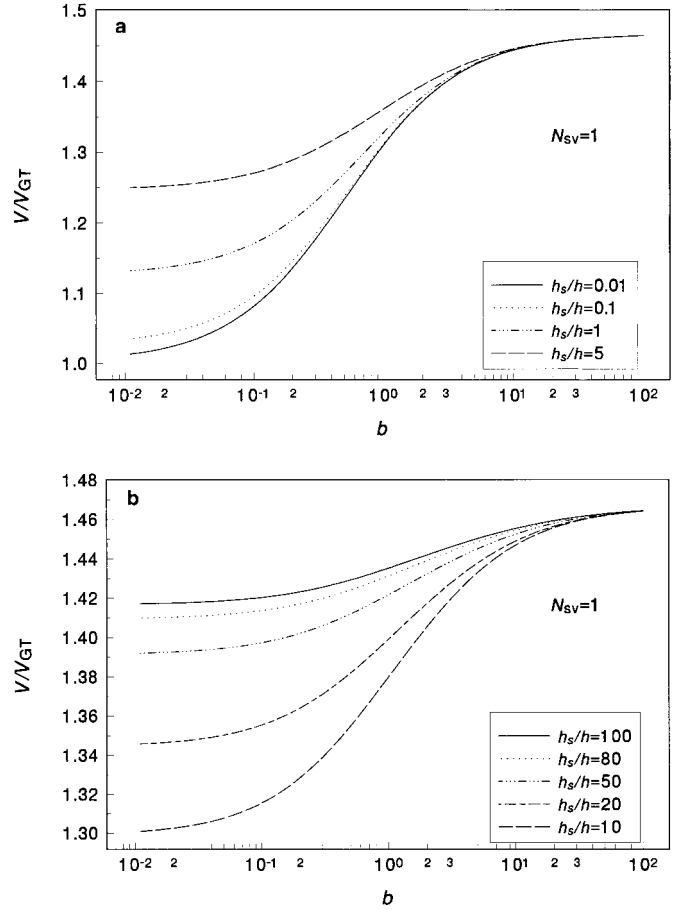


**FIG. 5.** Dimensionless approaching velocity,  $V/V_{GT}$ , as a function of the bulk diffusion parameter  $b$ : (a) for  $N_{sv} = 1$  and low and moderate surface diffusivities; (b) for  $N_{sv} = 1$  and high surface diffusivity.

when the bulk diffusion coefficient is smaller (the limiting case being an insoluble surfactant). If  $b$  is large enough all curves merge, which corresponds to finite values of surface viscosity number without any influence of interfacial elasticity (see Figs. 5a and 5b). Such a behavior is possible only for very low surfactant concentrations when the Gibbs elasticity is so low that it does not influence the mobility of the interfaces.

#### 4. EFFECT OF THE SURFACE PROPERTIES AND THE MENISCUS ON THE FILM DRAINAGE

In the case (B) of well-defined plane-parallel film with meniscus the solution of the problem [20] is described below. The analytical formulas obtained in Section 4.2 help us to estimate the influence of physical parameters in the particular cases of small or large surface viscosity. The numerical analysis is described in Section 4.3.

##### 4.1. Exact Solution of the Problem

Most of the experimental and theoretical investigations showed that after the film formation due to the disjoining and

capillary pressure the film drains without significant changing of its radius and shape of the interfaces (19, 20, 25, 31). Then the local film thickness can be approximated with a high precision as corresponding to the gap between two spherical segments separated by a planar region (see Fig. 1b):  $\tilde{H} = 1$  when  $0 \leq x \leq N_{\text{rf}}$ , and  $\tilde{H} = 1 - N_{\text{rf}}^2 + x^2$  when  $x \geq N_{\text{rf}}$ , where the dimensionless parameter  $N_{\text{rf}} \equiv R/\sqrt{R_c h}$  characterizes the film radius,  $R$ . It is not convenient to calculate the solution of [20] in terms of the variable  $x$ , because of the infinity point (see discussions in the previous section). Therefore, we introduce a new variable  $x = N_{\text{rf}} \tan(\zeta/2)$  in which the planar and meniscus regions transform into numerical domains with one and the same length:  $0 \leq \zeta \leq \pi/2$ , the planar region, and  $\pi/2 \leq \zeta \leq \pi$ , the meniscus region. Then the computations in the new variable account for both regions in a comparable way. Equation [20a] can be written in the new variable as

$$N_{\text{sv}} \sin^2(\zeta) \frac{\partial^2 \tilde{U}}{\partial \zeta^2} + N_{\text{sv}} \sin(\zeta) \cos(\zeta) \frac{\partial \tilde{U}}{\partial \zeta} - \left[ N_{\text{sv}} + \left( \frac{1}{\tilde{H}} + \frac{h}{h_s + hb\tilde{H}} \right) N_{\text{rf}}^2 \tan^2\left(\frac{\zeta}{2}\right) \right] \tilde{U} = - \frac{1}{\tilde{H}^2} \left[ N_{\text{rf}} \tan\left(\frac{\zeta}{2}\right) \right]^3. \quad [25]$$

Following the idea of Section 3.1, it is convenient to represent the solution of [25] as a Fourier series  $\tilde{U} = \sum_{k=1}^{\infty} b_k \sin(k\zeta)$ , which obeys the boundary conditions at the film center and at infinity:  $\tilde{U}(t, 0) = 0$  and  $\tilde{U}(t, x) \rightarrow 0$  at  $x \rightarrow \infty$ . The coefficients,  $b_k$ , depend implicitly on time. The description of the numerical procedure for equation [25] is given in Appendix B. After the computation of the coefficients, the Fourier expansion is substituted in [20b] and the final value of the drainage velocity is calculated numerically.

#### 4.2. Analytical Solutions in the Cases of Small and Large Surface Viscosity Number

When the surface viscosity is very low we can neglect all terms proportional to  $N_{\text{sv}}$ . The problem [20] has the following analytical solution

$$\tilde{U} = \frac{x}{\tilde{H}^2} \left( \frac{1}{\tilde{H}} + \frac{h}{h_s + hb\tilde{H}} \right)^{-1}, \quad [26a]$$

$$\frac{V_{\text{GR}}}{V} = \frac{1}{1 + b + h_s/h} + \frac{2h}{N_{\text{rf}}^4 h_s} \times \left\{ \left[ \frac{h}{h_s} (1 + b)(1 - N_{\text{rf}}^2) + 1 \right] \times \ln \left( 1 + \frac{h_s}{h(1 + b)} \right) + N_{\text{rf}}^2 - 1 \right\}, \quad [26b]$$

where  $V_{\text{GR}} = 2h^3 F_{\text{hd}} / (3\pi\eta R^4)$  is the generalized Reynolds' result for the rate of thinning of a fluid layer between two rigid plane-parallel circular disks with radii  $R$  (6), which takes into account the influence of the disjoining pressure. The first order correction of the velocity of film thinning proportional to the surface viscosity number  $N_{\text{sv}}$  is given in Appendix C.

When the surfactants are insoluble then in [26a] the bulk diffusion parameter is replaced by zero. In the particular case of infinite plane-parallel film,  $N_{\text{rf}} \gg 1$ , when the influence of meniscus can be neglected, the relationship [26b] is simplified to the result of Radoev *et al.* (15):  $V/V_{\text{GR}} = 1 + b + h_s/h$ . In the other limiting case of tangentially immobile interfaces (large Gibbs elasticity) Eq. [26b] is transformed to the following simple relation between the drainage velocity and the generalized Taylor and Reynolds velocities,

$$\frac{1}{V} = \frac{1}{V_{\text{GR}}} + \frac{1}{V_{\text{GT}}} + \frac{1}{\sqrt{V_{\text{GR}} V_{\text{GT}}}}, \quad [27a]$$

or, in equivalent form,

$$\frac{V_{\text{GT}}}{V} = 1 + \frac{R^2}{hR_c} + \frac{R^4}{h^2 R_c^2} \equiv 1 + \frac{h_i}{h} + \frac{h_i^2}{h^2}, \quad [27b]$$

where  $h_i$  is the so called inversion thickness. When  $h_i$  is reached the interfacial shape in the gap changes from convex to concave. The relationships [27a] and [27b] show that for small film radius,  $R$ , the drainage velocity reduces to the generalized Taylor velocity, whereas for large films,  $R^2/(hR_c) \gg 1$ , it yields the generalized Reynolds velocity. From [27b] it is seen also that when the film thickness is close to the inversion thickness,  $h_i$ , the generalized Taylor and Reynolds velocities have the same order of magnitude. Therefore, the meniscus influences the whole process of film drainage.

The other limit is the case of high surface viscosity, i.e.,  $N_{\text{sv}}/N_{\text{rf}}^2 \gg 1$ ,  $N_{\text{sv}}h_s/(N_{\text{rf}}^2 h) \gg 1$ , and  $N_{\text{sv}}b/N_{\text{rf}}^2 \gg 1$ . If we compare these inequalities with the corresponding ones in Section 3.2, we see that the larger the film radius is the more strict are the limit of applicability of the assumptions. For very large films the influence of surface viscosity on their thinning can be neglected. In this case equation [20] has an exact solution: in the film region it is

$$\tilde{U} = \frac{x}{8N_{\text{sv}}} (N_{\text{rf}}^2 - x^2) + \tilde{U}_R \frac{x}{N_{\text{rf}}}, \quad [28a]$$

and in the meniscus region it is

$$\tilde{U} = \tilde{U}_R \frac{N_{\text{rf}}}{x} + \frac{1}{4N_{\text{sv}}} \frac{1}{x} \ln(1 + x^2 - N_{\text{rf}}^2), \quad [28b]$$

where  $\tilde{U}_R$  is the unknown velocity at the film ring ( $r = R$ ;  $x = N_{\text{rf}}$ ). The first derivatives with respect to  $x$  of both solutions

[28a] and [28b] at the film ring have to be equal; therefore, for the velocity we obtain  $\tilde{U}_R = N_{rf}(N_{rf}^2 + 2)/(8N_{sv})$ . The exact solution [28] of the problem is continuous up to the third derivative of the function at  $x = N_{rf}$ . It is interesting to discuss the validity of the boundary conditions used in the literature for deriving the solution of the corresponding problem in the case of finite plane-parallel film. It is easy to find that: (i) the boundary condition  $\partial\tilde{U}/\partial x = 0$  at the film ring, used in Ref. 13, is valid only for  $N_{rf} = \sqrt{2}$  and (ii) the boundary condition used in Ref. 12 states that the fluctuation of the surfactant concentration should be equal to zero. It is easy to show that this boundary condition is equivalent to  $\partial(x\tilde{U})/\partial x = 0$ . This condition is also inapplicable. In the case of small surface viscosity we performed an asymptotic analysis of the problem. We established that the boundary layer at the film ring,  $x = N_{rf}$ , is very thin; its thickness,  $\delta_{fr}$ , is approximately  $\delta_{fr} = \sqrt{N_{sv}(1+a)}$ , where the dimensionless parameter,  $a$ , is defined as  $a \equiv h/(h_s + bh)$ . The theory of singular perturbations was applied and the value of the velocity derivative at the film ring was found to be

$$\frac{\partial\tilde{U}}{\partial x} = \frac{1}{1+a} + N_{rf}^2 \frac{ba^2 - 2a - 1}{(1+a)^2}.$$

Therefore, the boundary condition  $\partial\tilde{U}/\partial x = 0$  at the film ring, used in Ref. 13, is valid only for the particular case  $N_{rf}^2 = (1+a)/(2a+1-ba^2)$ .

After substitution of [28] into the general formula [20b] the final result for the velocity of thinning reads

$$\frac{1}{V} = \left[ \frac{1}{V_{GT}} + \frac{1}{V_{GR}} + \frac{1}{\sqrt{V_{GT}V_{GR}}} - \frac{1}{2N_{sv}} \right. \\ \left. \times \left( \frac{1}{V_{GT}} + \frac{1}{V_{GR}} + \frac{1}{\sqrt{V_{GT}V_{GR}}} + \frac{N_{rf}^2}{3\sqrt{V_{GT}V_{GR}}} \right) \right]. \quad [29]$$

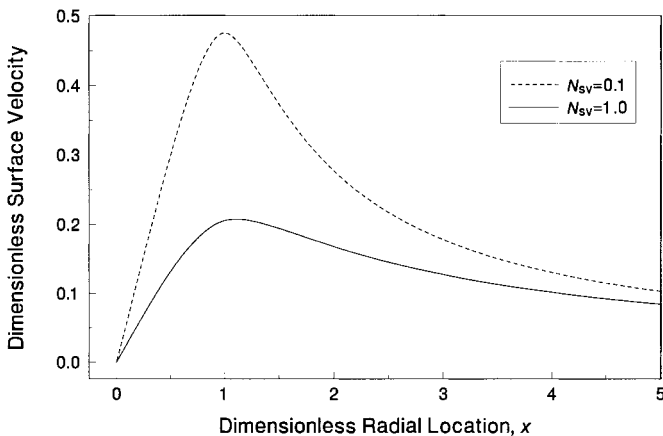


**FIG. 6.** Dimensionless surface velocity,  $\tilde{U}$ , distribution at a given distance  $x$  for  $b = 1$ ,  $h_s/h = 1$ ,  $N_{rf} = 1$  and different values of the parameter  $N_{sv}$ .

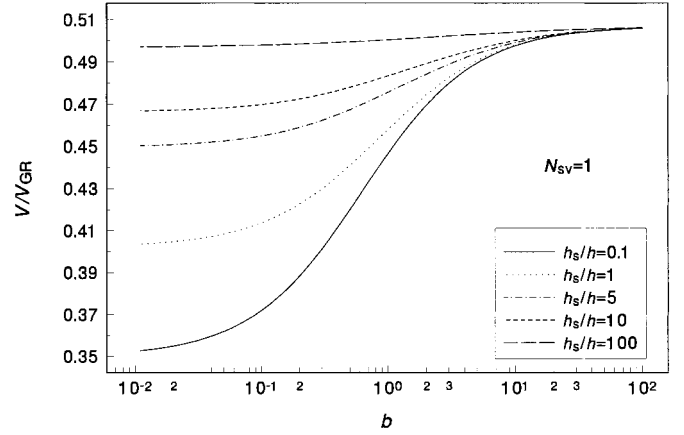


**FIG. 7.** Variation of the mobility factor,  $V/V_{GR}$ , with the bulk diffusion parameter  $b$  for  $N_{sv} = 1$ ,  $N_{rf} = 1$  and different values of  $h_s/h$ .

This relationship is the generalization of [27] for large surface viscosity.

### 4.3. Numerical Results and Discussions

The numerical procedure used for the calculations given below is described in Appendix B. The effect of surface viscosity on the interfacial mobility is plotted in Fig. 6. If the bulk and surface diffusion coefficients,  $D$  and  $D_s$ , the distance between the bubbles,  $h$ , and the film radius,  $R$ , are constants, then with increasing of the surface viscosity number the surface mobility decreases. The distance where the dimensionless surface velocity has a maximum slightly decreases with increasing of  $N_{sv}$  and the interfaces are mobile in a wide meniscus region. From Fig. 6 it follows that the maximum of the surface velocity is achieved close to the film ring, but the influence of the meniscus on the drainage is not negligible.

In order to clarify the influence of the material interfacial properties on the velocity of film thinning we calculate the mobility factor  $V/V_{GR}$  for different values of  $b$ ,  $h_s/h$ , and  $N_{sv}$ ,

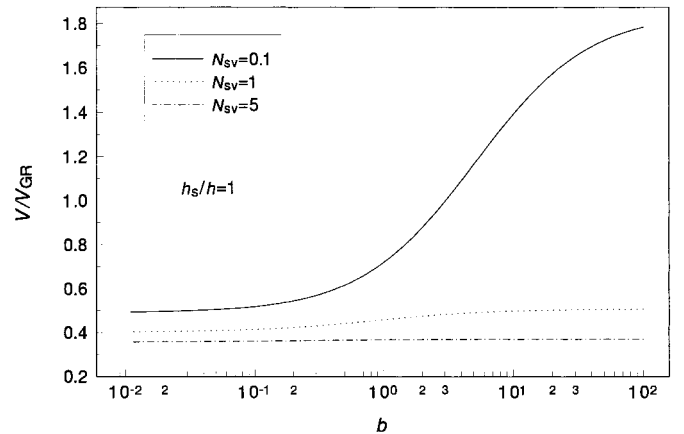


**FIG. 8.** Dimensionless velocity of film thinning,  $V/V_{GR}$ , as a function of the bulk diffusion parameter  $b$  for  $h_s/h = 1$ ,  $N_{rf} = 1$  and different values of surface diffusion number,  $N_{sv}$ .

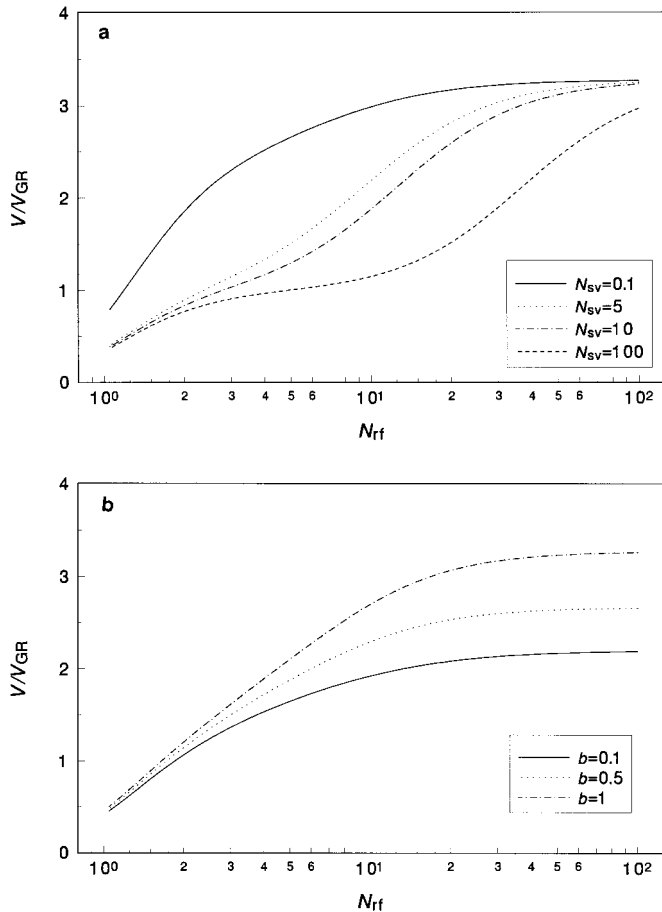


**FIG. 9.** Variation of the mobility factor,  $V/V_{GR}$ , with the dimensionless film radius,  $N_{rf}$ : (a)  $b = 1$ ,  $h_s/h = 1$  and different surface viscosities; (b)  $N_{sv} = 1$ ,  $h_s/h = 1$  and different bulk diffusivities.

keeping the film radius,  $R$ , and the film thickness,  $h$ , constant. Fig. 7 illustrates the dependence of  $V/V_{GR}$  on the bulk diffusion number,  $b$ , at different surface diffusion coefficients and  $N_{sv} = 1$ . The increase of  $h_s/h$  leads to increasing velocity of thinning. The interfaces behave as more mobile, because of suppression of the Marangoni effect: at faster surface diffusion the distribution of surfactant on the interface is closer to the equilibrium. This effect is more pronounced when the surfactants behave as insoluble, for smaller values of the bulk diffusion parameter  $b$ . For the higher bulk diffusivity all curves merge corresponding to values of surface viscosity number ( $N_{sv} = 1$ ) without any influence of surface diffusivity (see Fig. 7). In Fig. 8 the mobility factor was calculated for constant surface diffusion parameter  $h_s/h = 1$ . The higher the surface viscosity the slower the film drainage. The increase of the interfacial mobility due to the faster bulk diffusion is well pronounced for small surface viscosity. It is important to note that Figs. 7 and 8 show smaller drainage velocity,  $V$ , than the generalized Reynolds velocity,  $V_{GR}$ , in the cases when the surface viscosity is not so low. This effect is exactly due to the influence of the meniscus: the additional hydrodynamic resistance of the meniscus can be larger or comparable with the friction in the plane parallel film region.

It is interesting to estimate the influence of the geometrical parameters of the system on the velocity of film thinning. In order to do that, we calculate the mobility factor  $V/V_{GR}$  for different values of film radius,  $R$ . In our computation we kept all physical dimensionless parameters constant (they do not depend on  $R$ ), except the number  $N_{rf}$ . In the literature (14) it is proved that the film is formed when the distance between the bubbles is equal to the inversion thickness,  $h_i$ ; in this case  $N_{rf} \propto 1$ . Therefore, the values of  $N_{rf}$  can be larger or much larger than 1, because the smaller the thickness  $h$  the larger the parameter  $N_{rf}$ . It is seen from Fig. 9 that the decrease of the film thickness (respectively, with increasing film radius,  $R$ , for example in the Sheludko cell where the films can be with different radii) leads to increasing velocity of thinning. This effect is a combination of two reasons, which lead to the same behavior. The first one is the decreasing of the relative influence of the meniscus at larger film radii (the main hydrodynamic friction is concentrated in the plane-parallel film region). The second reason is connected with the circumstance that for a wide range of values for surface viscosity the influence of elasticity and bulk and surface diffusivities in the whole process of film thinning is well pronounced depending on the film radius (see Fig. 9). This fact is proved also for very high surface viscosity number  $N_{sv} = 100$ , and for large values of  $N_{rf}$ . This effect was mentioned by Ivanov *et al.* (12) and Singh *et al.* (13), who showed that for large plane-parallel films the velocity of thinning depends not on  $N_{sv}$ , but on the complex ratio between the dimensionless parameters  $N_{sv}(h_s/h + b)/[N_{rf}^2(1 + h_s/h + b)]$ . Therefore, the relative influence of the surface viscosity decreases strongly with increasing of the film radius,  $R$ , or with the decrease of the film thickness,  $h$ . In other words, for large films the mobility of the interfaces in the plane-parallel region can depend only on the bulk and surface diffusivities. The influence of bulk diffusion is illustrated in Fig. 9b, where the other dimensionless numbers are  $h_s/h = 1$  and  $N_{sv} = 1$ . It is seen that with increasing of the film radius the mobility of the interfaces increases. The asymptotic value of the relative velocity at  $N_{rf} = 100$  is exactly the same as that given by Eq. [26b].

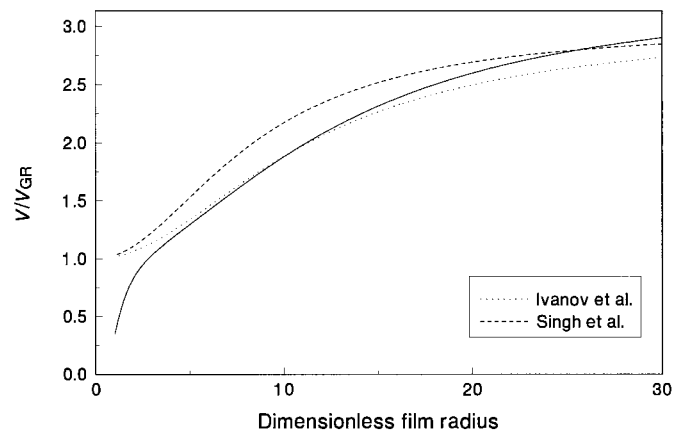


**FIG. 10.** Comparison of the mobility factor  $V/V_{GR}$  as predicted by Ivanov *et al.* (12) and Singh *et al.* (3) for finite plane-parallel film and our model. The parameters in the calculations are  $b = 1$ ,  $h_s/h = 1$  and  $N_{sv} = 10$ .

In Section 4.2 we discussed the correctness of the boundary conditions used in Refs. 12 and 13 for solving the problem of plane-parallel thin liquid film drainage. We also demonstrated that for large film radii the influence of the meniscus on the drainage velocity can be neglected. It is interesting to check if the boundary conditions are so important for large films. The result of Ref. 12 for the relative velocity can be presented in terms of our dimensionless parameters as

$$\frac{V}{V_{\text{Re}}} = \frac{1}{16} \left[ \sum_{k=1}^{\infty} \frac{2}{\lambda_k^4} \frac{1 + N_{\text{sv}} \lambda_k^2 (b + h_s/h) / N_{\text{rf}}^2}{1 + (b + h_s/h) (1 + N_{\text{sv}} \lambda_k^2 / N_{\text{rf}}^2)} \right]^{-1}, \quad [30]$$

where  $\lambda_k$  is the  $k$ th zero of the zeroth order Bessel function,  $J_0(\lambda_k) = 0$ , and  $V_{\text{Re}}$  is the Reynolds velocity. The corresponding result from Ref. 13 can be written in the form

$$\frac{V}{V_{\text{Re}}} = \left[ \frac{1}{1 + b + h_s/h} + \frac{4N_{\text{sv}}}{N_{\text{rf}}^2} \left( \frac{b + h_s/h}{1 + b + h_s/h} \right)^2 \frac{2I_1(\xi) - \xi I_0(\xi)}{I_1(\xi) - \xi I_0(\xi)} \right]^{-1}, \quad [31]$$

where  $I_0$  and  $I_1$  are the modified Bessel functions and the parameter  $\xi$  is defined as

$$\xi = \left( \frac{N_{\text{rf}}^2}{N_{\text{sv}}} \frac{1 + b + h_s/h}{b + h_s/h} \right)^{1/2}.$$

The numerical calculations for the relative velocity of thinning from our model and from the formulas [30] and [31] are given in Fig. 10. The parameters are  $b = 1$ ,  $h_s/h = 1$ , and  $N_{\text{sv}} = 10$ . It is well demonstrated that with increasing the film radius the results from our model go to the results of Ivanov *et al.* (12) and Singh *et al.* (13), which are not significantly different. For small film radius the drainage velocity is smaller due to the influence of the meniscus. Therefore, for large films the boundary condition  $\partial \tilde{U} / \partial x = 0$  at the film ring seems to be more realistic than the boundary condition  $\partial(x\tilde{U}) / \partial x = 0$  (see Ref. 33). The latter one provides a negative first derivative of the velocity at the film ring. Then the maximum of the velocity is somewhere inside the film, the viscous friction is larger than the real one, and therefore the drainage velocity is smaller.

## 5. CONCLUSIONS

1. A theoretical model for calculation of the influence of surfactants on the approaching velocity of two nondeformed bubbles is developed. It takes into account the influence of Gibbs elasticity, bulk and surface diffusivities, and surface viscosity. The governing equation for the surface velocity is calculated numerically in order to find the velocity of approach, relative to the generalized Taylor velocity. In the case of small and large surface viscosity numbers the derived analytical formulas [23b] and [24b] are useful for a simple approximation of the velocity.

2. The quantitative calculations show that with an increase of the surface viscosity the interfaces become immobile. The same behavior is observed also with an increase of the Gibbs elasticity. This effect takes place only for moderate values of the bulk and surface diffusivities. The increase of the bulk diffusion coefficient leads to faster saturation of the interfaces, which contrabalances the surface gradient of surfactant, suppresses the Marangoni effect, and makes the interfaces mobile (see Figs. 4 and 5). The surface diffusion effect is the dominant factor compared to the bulk diffusion, especially for very thin films where  $h_s/h$  can be large or on the order of unity, whereas  $b$  is a small parameter.

3. In the case of plane-parallel film with a meniscus region the developed model is based on the spherical approximation of the meniscus profile. The calculations are carried out using the whole film profile. The correctness of the previous results (12, 13) are discussed. It is shown that the approximation of the film as composed of only a finite plane-parallel part gives good results when the dimensionless film radius is large enough. In this case the boundary conditions for the surface velocity at the film ring are not so important for the final value of the velocity of film thinning relative to the Reynolds velocity. Then the main parameter which estimates the influence of surface viscosity is proved to be  $N_{\text{sv}}(h_s/h + b) / [N_{\text{rf}}^2(1 + h_s/h + b)]$ .

4. The asymptotic results for large and small surface velocity, Eqs. [26b], [27], and [29], give simple analytical relationships for calculation of the drainage velocity. They predict a continuous transition from the deformed to the nondeformed bubbles approximation. The numerical results from this problem show a significant influence of the meniscus region on the drainage velocity. The latter can be smaller than the common Reynolds velocity and the drainage of the film between small drops and bubbles can be slower.

## APPENDIX A

### Numerical Solution of the Problem [21]

The problem [21] can be written in the following form:

$$\begin{aligned} N_{\text{sv}} & \left[ -\cos(3\theta) - 2 \left( 2 \frac{h}{h_s} b + 1 \right) \cos(2\theta) \right. \\ & \left. + \cos(\theta) + 2 \left( 2 \frac{h}{h_s} b + 1 \right) \right] \frac{\partial^2 \tilde{U}}{\partial \theta^2} \\ & + N_{\text{sv}} \left[ \sin(3\theta) + 2 \left( 2 \frac{h}{h_s} b + 1 \right) \sin(2\theta) + \sin(\theta) \right] \frac{\partial \tilde{U}}{\partial \theta} \\ & + \left[ \cos(2\theta) - 4 \left( N_{\text{sv}} - \frac{h}{h_s} b - \frac{h}{h_s} \right) \cos(\theta) + 1 \right. \\ & \left. - 4 \frac{h}{h_s} - 2(2N_{\text{sv}} + 1) \left( 2 \frac{h}{h_s} b + 1 \right) \right] \tilde{U} \\ & = \frac{1}{4} \sin(3\theta) + \frac{h}{h_s} b \sin(2\theta) - \left( 2 \frac{h}{h_s} b + \frac{3}{4} \right) \sin(\theta). \quad [A.1] \end{aligned}$$

After substitution of the Fourier series  $\tilde{U} = \sum_{k=1}^{\infty} a_k \sin(k\theta)$  into Eq. [A.1] we derive an infinite linear system of equations for the unknown quantities  $a_k$ . The coefficients in this system are complex functions of the physical parameters and they will not be presented here. This system is of seven-diagonal type and is solved numerically by means of the Thompson algorithm. The special type of the system gives us the possibility to solve the problem for a large number of coefficients (in our calculations the cut off number was 10,000).

## APPENDIX B

### Numerical Solution of the Problem [25]

For the numerical solution of Eq. [25] we cannot use the same procedure as in the Appendix A, because the shape function cannot be presented as a finite Fourier series. That is why all coefficients in the respective linear system of equations are different from zero. We used the functional Ritz numerical methods (32). For that purpose the Fourier series  $\tilde{U} = \sum_{k=1}^{\infty} b_k \sin(k\zeta)$  is substituted into Eq. [25], the result is multiplied by  $\sin(n\zeta)$  and is integrated from 0 to  $\pi$ . The final infinite linear system of equations for the unknown coefficients reads

$$\sum_{k=1}^{\infty} a_{n,k} b_k = d_n, \quad \text{for } n = 1, 2, \dots \quad [\text{B.1}]$$

In Eq. [B.1] the coefficients  $a_{n,k}$  and  $d_n$  are calculated from the following relationships:

$$a_{n,k} = \int_0^{\pi} \{N_{\text{sv}} [k^2 \sin^2(\zeta) \sin(k\zeta) - k \sin(\zeta) \cos(\zeta) \cos(k\zeta) + \sin(k\zeta)] + \left(\frac{1}{\tilde{H}} + \frac{h}{hb\tilde{H} + h_s}\right) N_{\text{rt}}^2 \tan^2\left(\frac{\zeta}{2}\right) \sin(k\zeta)\} \sin(n\zeta) d\zeta, \quad [\text{B.2}]$$

$$d_n = \int_0^{\pi} \frac{1}{\tilde{H}^2} \left[ N_{\text{rt}} \tan\left(\frac{\zeta}{2}\right) \right]^3 \sin(n\zeta) d\zeta. \quad [\text{B.3}]$$

For our calculations we used the Gauss–Jordan elimination method (32) in which the cut off number of equations was 50. We checked also that this number was enough to calculate the relative velocity with a good precision.

## APPENDIX C

### Asymptotic Solution for Small Surface Viscosity

Here we present the final analytical results for the first order series expansion of the velocity of approach of two nonde-

formed bubbles in the case of small surface viscosity number,  $N_{\text{sv}} \ll 1$ ,

$$\frac{V_{\text{GT}}}{V} = \frac{2h}{h_s} \left[ \left( \frac{1}{N_d} + 1 \right) \ln(N_d + 1) - 1 \right] + 8N_{\text{sv}} \left\{ \frac{1}{3} + \frac{1}{3} \frac{1}{(b+1)^3 (N_d+1)^2} + \frac{2(N_d+1)}{N_d^2(b+1)} \left[ \frac{2}{N_d} \ln(N_d+1) - \frac{N_d+2}{N_d+1} \right] \right\}, \quad [\text{C.1}]$$

where the dimensionless parameter  $N_d$  is defined as

$$N_d \equiv \frac{h_s}{h(b+1)}. \quad [\text{C.2}]$$

It is seen that the term proportional to  $N_{\text{sv}}$  depends only on the bulk diffusion parameter  $b$  and on the ratio  $N_d$ .

The corresponding formula in the case (B) for deformed bubbles is very complicated. Therefore, here we will report the particular case for large film radius or small film thickness. The final result reads

$$\frac{V_{\text{GR}}}{V} = \frac{1}{1+b+h_s/h} + 8N_{\text{sv}} \left\{ \frac{1}{3} + \frac{1}{3} \frac{1}{(b+1)^3 (N_d+1)^4} + \frac{2}{N_d^2(b+1)} \left[ \frac{2}{N_d} \ln(N_d+1) - \frac{N_d+2}{N_d+1} \right] - \frac{b+N_d(b+1)}{(b+1)^2 (N_d+1)^2} \left[ \frac{N_d}{N_d+1} + (b+1) \left( N_d + \frac{b}{b+1} \right) \right] \right\}. \quad [\text{C.3}]$$

As in the previous case the first approximation of the relative velocity depends on the bulk diffusivity number  $b$  and the parameter  $N_d$ .

## ACKNOWLEDGMENT

This work was funded by the Inco-Copernicus Project PL979098. The authors are grateful for this financial support.

## REFERENCES

1. Behcer, P., Ed., "Encyclopedia of Emulsion Technology." Marcel Dekker, New York, 1996.
2. Prud'home, R. K., and Khan, S. A., Eds., "Foams, Theory, Measurements, and Applications." Marcel Dekker, New York, 1996.
3. Bancroft, W. D., *J. Phys. Chem.* **17**, 514 (1913).
4. Griffin, J., *Soc. Cosmet. Chem.* **5**, 4 (1954).
5. Schinoda, K., and Friberg, S., "Emulsion and Stabilization." Wiley, New York, 1986.
6. Ivanov, I. B., *Pure Appl. Chem.* **52**, 1241 (1980).

7. Plateau, J., *Mem. Acad. Roy. Soc. (Belgium)* **37**, 1 (1869).
8. Marangoni, C. G. M., *Ann. Physik. (Poggendorff)* **3**, 337 (1871).
9. Boussinesq, N., *Ann. Chim. Phys.* **29**, 349 (1913).
10. Saboni, A., Gourdon, C., and Chester, A. K., *J. Colloid Interface Sci.* **175**, 27 (1995).
11. Rother, M. A., Zinchenko, A. Z., and Davis, R. H., *J. Fluid Mech.* **346**, 117 (1997).
12. Ivanov, I. B., and Dimitrov, D. S., *Colloid Polym. Sci.* **252**, 982 (1974).
13. Singh, G., Hirasaki, G. J., and Miller, C. A., *J. Colloid Interface Sci.* **184**, 92 (1996).
14. Ivanov, I. B., Dimitrov, D. S., Somasundaran, P., and Jain, R. K., *Chem. Eng. Sci.* **40**, 137 (1985).
15. Radoev, B. P., Dimitrov, D. S., and Ivanov, I. B., *Colloid Polym. Sci.* **252**, 50 (1974).
16. Zapryanov, Z., Malhotra, A. K., Aderangi, N., and Wasan, D. T., *Int. J. Multiphase Flow* **9**, 105 (1983).
17. Tambe, D. E., and Sharma, M. M., *J. Colloid Interface Sci.* **147**, 137 (1991).
18. Ivanov, I. B., Radoev, B. P., Traykov, T., Dimitrov, D., Manev, E., and Vassilieff, Chr., in "Proceedings of the International Conference on Colloid and Surface Science" (E. Wolfram, Ed.), Vol. 1, p. 583. Akademia Kiado, Budapest, 1975.
19. Ivanov, I. B., and Dimitrov, D. S., in "Thin Liquid Films" (I. B. Ivanov, Ed.), p. 379. Dekker, New York, 1988.
20. Denkov, N. D., Petsev, D. N., and Danov, K. D., *J. Colloid Interface Sci.* **176**, 189 (1995).
21. Kralchevsky, P. A., Danov, K. D., and Denkov, N. D., in "Handbook of Surface and Colloid Chemistry" (K. S. Birdi, Ed.), p. 333. CRC Press, New York, 1997.
22. Taylor, P., *Proc. Roy. Soc. (London) A* **108**, 11 (1924).
23. Reynolds, O., *Phil. Trans. Roy. Soc. (London) A* **177**, 157 (1886).
24. Scheludko, A., *Adv. Colloid Interface Sci.* **1**, 391 (1967).
25. Barber, A. D., and Hartland, S., *Can. J. Chem. Eng.* **54**, 279 (1976).
26. Li, D., *J. Colloid Interface Sci.* **163**, 108 (1994).
27. Traykov, T. T., and Ivanov, I. B., *Int. J. Multiphase Flow* **3**, 471 (1977).
28. Traykov, T. T., Manev, E. D., and Ivanov, I. B., *Int. J. Multiphase Flow* **3**, 485 (1977).
29. Malhotra, A. K., and Wasan, D. T., *AIChE J.* **33**, 1533 (1987).
30. Davis, R. H., Schonberg, J. A., and Rallison, A. M., *Phys. Fluids* **A1**, 77 (1989).
31. Velev, O. D., Constantinides, G. N., Avraam, D. G., Payatakes, A. C., and Borwankar, R. P., *J. Colloid Interface Sci.* **175**, 68 (1995).
32. Press, W. H., Teukolsky, S. A., Vetterling, W. T., and Flannery, B. P., "Numerical Recipes in FORTRAN. The Arts of Scientific Computing." Cambridge University Press, 1992.
33. Singh, G., Ph.D. Thesis, Rice University, 1996.